

Knotted Strapwork Strands in a Penrose-Type Girih Pattern

Joseph I. Cline

Department of Chemistry, University of Nevada, Reno, USA; cline@unr.edu

Abstract

The properties of selected knotted strapwork strands emergent in a Girih decoration of an aperiodic Penrose P2 tiling are quantified. The selected strands are from six families with distinctive shapes and knot topology. Although it is not evident how to predict strand properties *a priori*, and despite the evolution of fractal structures, many features of these strand families follow quantitative scaling laws arising from the characteristics of Penrose tilings.

Introduction

This paper describes strands in decorative strapwork that obey a common “golden rule” observed in traditional Girih patterns found in Islamic tilings: the strapwork never bends at crossing intersections, and there are no terminations or “T” intersections [2][3]. When realized in three dimensions, this strapwork is interlaced such that every strand has alternating “over” and “under” strapwork crossings along its trajectory. The work of Grünbaum and Shephard [8], extended by Ostromoukov [12], showed how every strand shape in the Girih strapwork of a periodic tiling can be analytically obtained from the Caley diagram for the Girih decoration on a single repeat unit. They observed that medieval Girih patterns decorating periodic tilings typically show fewer than 4 unique strand shapes in the strapwork pattern [8]. In contrast, recently I showed that application of a simple Girih decoration rule to the kite and dart tiles in an aperiodic Penrose P2 tiling results in an apparent infinite variety of strand shapes and sizes in the strapwork pattern [4]. I provided a qualitative description of a small number of these strands, demonstrating that some show an astonishing degree of intricacy. It was observed that many of these strands can be grouped into families with similar structural themes, showing a systematic evolution in size and often showing fractal development of certain features.

I remain unable to provide an *a priori*, analytic method comparable to that of Grünbaum and Shephard to fully predict the strand shapes emergent in a Girih-decorated Penrose tiling. Nonetheless, this paper provides empirical organizing principles that allow quantitative prediction of the properties of certain strapwork strand families, some reported in [4], along with their mathematical knot topology. As might be expected, these organizing principles echo the remarkable properties of the well-known Penrose tiling and provide insight into its long-range structure. I also introduce a systematic nomenclature allowing unambiguous identification and location of individual strands within the Girih pattern.

Penrose Tiling and Girih Decoration Rule

We only consider a specific Girih decoration of a very large, though necessarily finite, region at the center of a “star axiom” Penrose P2 (kite and dart) tiling, as described in [4]. Though aperiodic, this tiling has $d5$ point group symmetry about the five-pointed star formed by the 5 darts sharing a vertex at its center. Figure 1(a,b) shows the kite and dart shapes, described elsewhere [5][6][7]. We define a to be the length of the long sides of the kites and darts, so that the short sides have length $\frac{a}{\phi}$, where ϕ is the Golden Ratio, $(1 + \sqrt{5})/2 \approx 1.6180$. In Figure 1(a,b) our Girih decoration rule is shown as black lines superimposed onto the kites and darts. Figure 1(c) shows a relatively tiny, $9a \times 9a$ region of the assembled, decorated star axiom tiling, centered on the point of $d5$ symmetry. The skeletal form of the resulting Girih pattern in Figure 1(c) omits the depiction of strapwork interlacing at strand crossings.

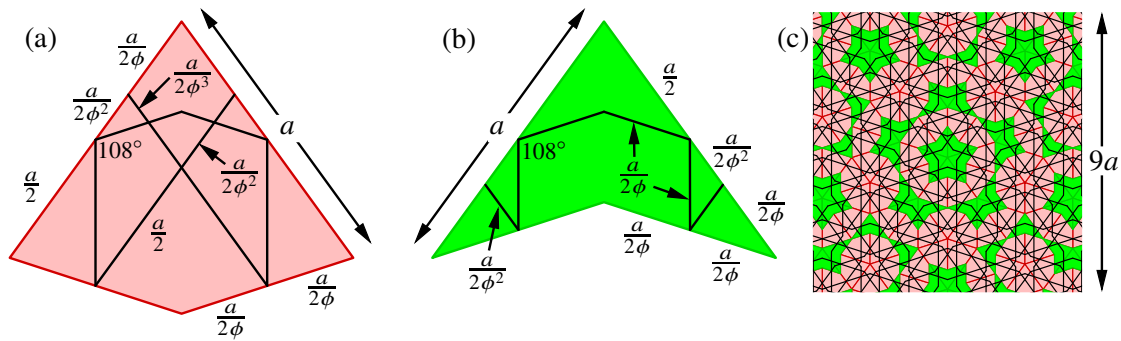


Figure 1: Girih decoration rule for the $P2$ tiling. (a) Kite with Girih decoration shown as black lines. (b) Decorated dart. (c) A decorated region of the tiling generated by inflation of the “star” vertex neighborhood [4]. The resulting tiling has $d5$ symmetry about the 5-pointed star at its center.

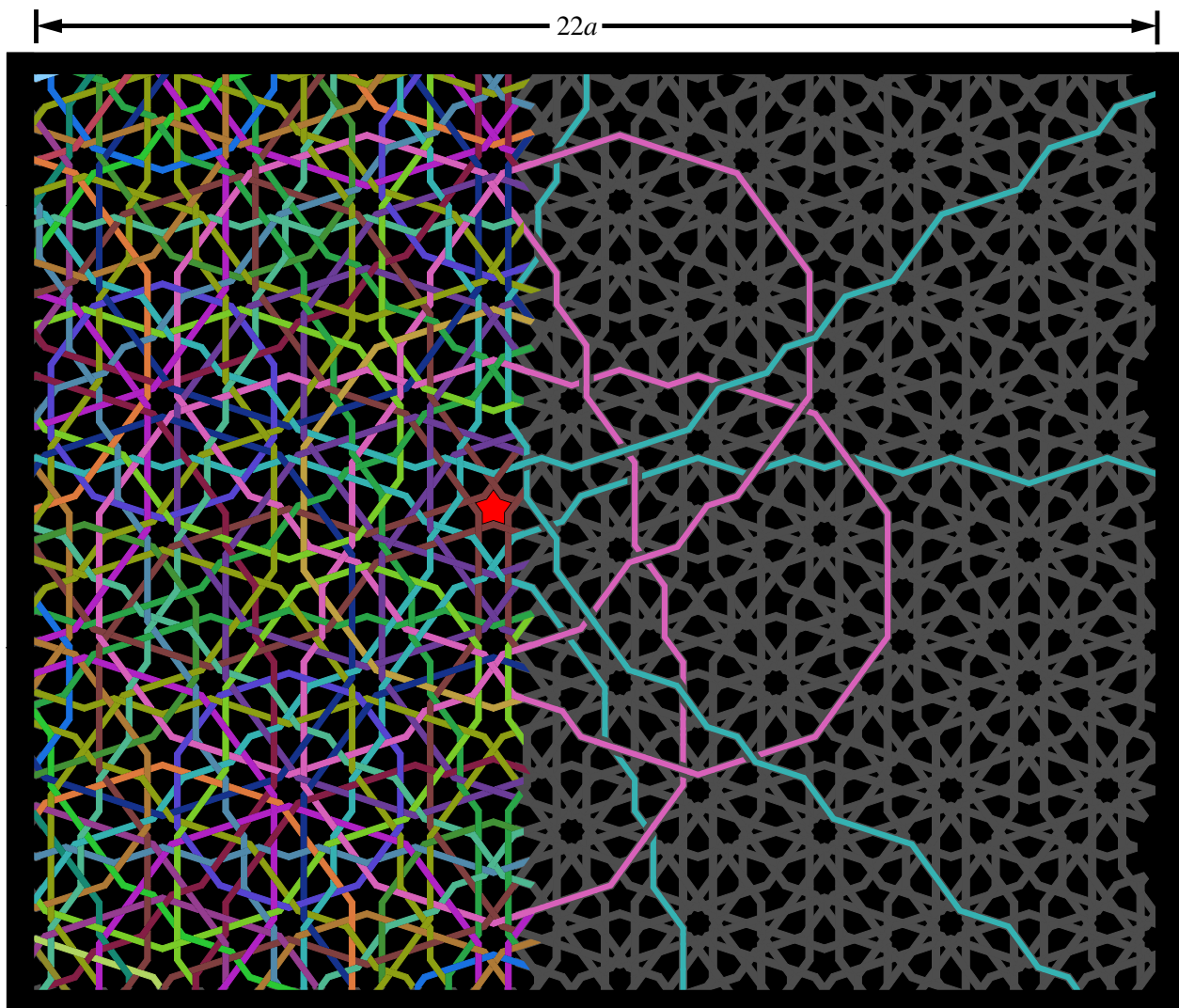


Figure 2: Decorated tiling with red star at the star axiom origin of the Cartesian coordinate system used to identify strand locations. Left: interwoven strapwork with a unique color for each strand. Right: skeletal Girih pattern with the $\{1, 3\}$ (pink) and $\{-1, 2\}$ (cyan) strands highlighted.

Figure 2 shows a slightly larger region of the Girih pattern, omitting depiction of the underlying kites and darts. For reference here and in subsequent figures, the $d5$ symmetry center of the Penrose tiling is highlighted as a 5-pointed red star. The left side of Figure 2 shows the alternate over and under strapwork crossings, with a unique color for each strand (or each symmetrically equivalent set of strands); the right side shows only the skeletal Girih pattern, excepting two selected strands which are highlighted as examples, discussed below. Strapwork interlacing generates chirality and destroys the tiling's $d5$ reflection planes; however the Girih pattern still has 5-fold rotation symmetry about the $d5$ symmetry center. Figure 2 shows one of the two possible mirror image Girih patterns. As in [4], selected strapwork strands are followed computationally, and all are observed to be closed loops. The symmetry of the Girih pattern dictates that all individual strands either have 5-fold rotational symmetry about the Penrose tiling's $d5$ symmetry center, or are members of a set of 5 identical strands interchanged by 72° rotations about the center.

Even within this small region, and despite the aid of color coding, it is tedious to visually follow the trajectory of an individual strand within the interwoven strapwork. Careful inspection reveals that most strands in Figure 2 escape the region depicted: strand trajectories often explore much larger regions of the tiling. Following the trajectory of the pink highlighted strand across both sides of Figure 2 shows that it forms a mathematical knot completely contained within the depicted region. As we will see, the cyan highlighted strand also has a knotted trajectory, but it escapes the region depicted in Figure 2.

These two highlighted strands are the smallest members of two different “strand families”, each having members of a characteristic shape and knot topology, but differing in size. In this paper we will report the properties of these two strand families, along with four other families of knotted strands. The strands considered here are only a small sampling of the bewildering variety of shapes and topologies observed in the strand survey of [4], many of which have far more complex and intricate trajectories. (See, for example, Figure 6 of [4].) For brevity and focus, the featured families in this report are constrained to those having individual member strands with 5-fold rotational symmetry about the $d5$ symmetry center of the star axiom Penrose tiling. As shown in [4], for families of this type, each successive member increases in size by approximately ϕ^2 and its orientation about the tiling center is rotated by 36° from its predecessor. Such strands have 5-fold rotational symmetry and in general may be chiral. It appears that such families have an infinite number of members. The number of strands that can be computationally tracked and that are described here is limited by the necessarily finite size of the tiling generated in [4], which had a usable radius of $a\phi^{17} \approx 3571a$ and contained approximately 49 million kites and 30 million darts.

Strand Analysis

We characterize each strand by a coordinate (b) giving its location within the star axiom tiling, the total number of crossings (N_c) encountered when completing the circuit of its trajectory through the interlaced Girih pattern, the number of self-crossings (N_s) of the strand with itself (note: N_c includes the self-crossings), the length (L) traversed in completing a circuit, and its knot topology. We locate individual strands on a Cartesian coordinate system with its origin at the center of the 5-pointed star axiom, and its $+y$ -axis directed toward a point of the star axiom. The reflection symmetry elements of the $d5$ point group dictate that every strand traversing the y -axis must have either a bend vertex or a self-crossing at the point of traversal.

Such a strand orbiting the center of the tiling can be uniquely identified by specifying the y -coordinate at any of its vertices or self-crossings when $x = 0$. Let b be the y -coordinate of one of these points of traversal (here chosen to be the innermost bend traversal and defined as the strand's “fiducial point”). Because the dimensions of the kites and darts and their Girih decorations (see Figure 1) are all a or $\frac{a}{2}$ multiplied by integral powers of $1/\phi$, one can use well-known identities relating integral powers of ϕ to show that $b = \frac{a}{2}(m_0 + \phi m_1)$, where m_0 and m_1 are integers unique to the chosen point of traversal. Every strand can then be located in the tiling strapwork by specification of a fiducial $\{m_0, m_1\}$ integer pair at its y -axis traversal fiducial point. Using

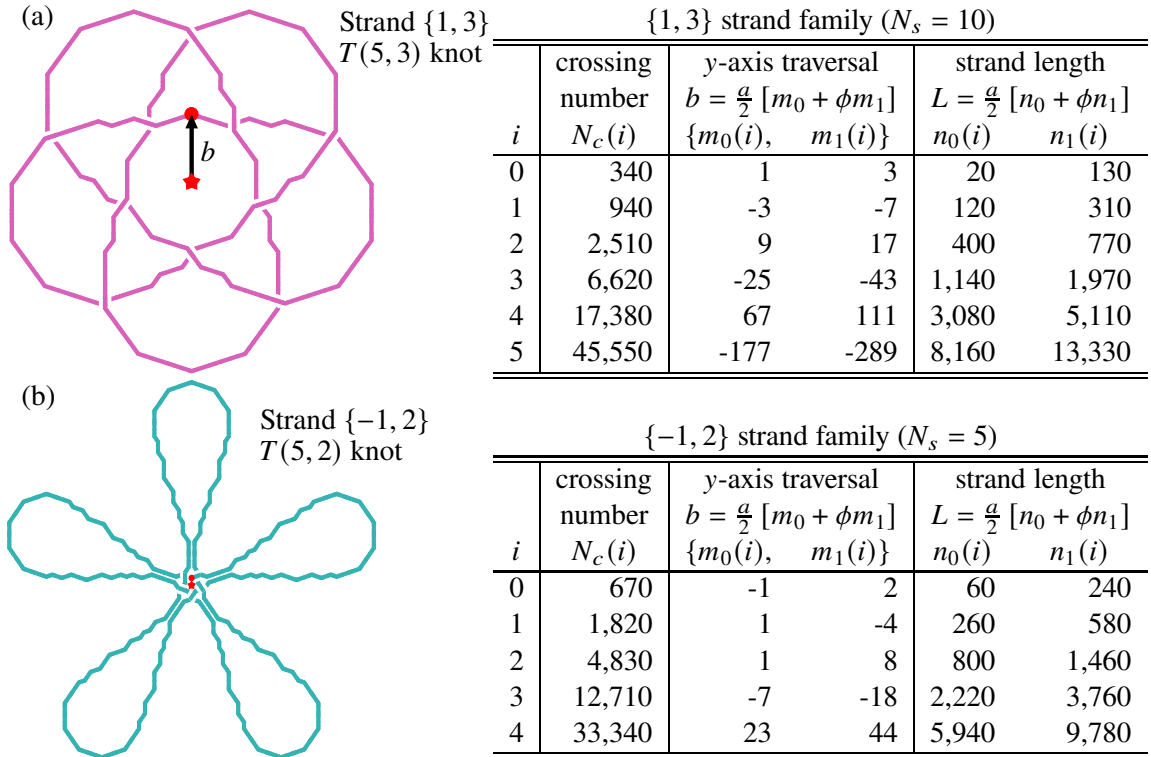


Figure 3: (a) First ($i = 0$) member of the $\{1, 3\}$ strand family and quantification of higher order members. (b) Same for $\{-1, 2\}$ family. The locations of strand fiducial points are labeled with red circles.

the same procedure to sum the lengths of a strand’s Girih segments shows that the total strand length can be expressed as $L = \frac{\alpha}{2} (n_0 + \phi n_1)$, where n_0 and n_1 are integers.

We now quantitatively characterize the properties of six strand families, identifying each member by a $\{m_0, m_1\}$ pair specifying its fiducial point location, and giving the n_0 and n_1 values for its length, L , and its crossing number, N_c . It is found that all members of a given strand family share the same knot topology and self-crossing number, N_s (with one exception to be discussed). Note that, in the language of knot theory, N_s is the crossing number of the strand’s knot projection onto the tiling plane, which in general is not guaranteed to be crossing number associated with its minimal knot projection [9].

The $\{1, 3\}$ family. The pink strand highlighted on the right side of Figure 2 is the “founding” ($i = 0$) member of the $\{1, 3\}$ family and has a crossing number $N_c(0) = 340$. It is located by the fiducial point $\{1, 3\}$ at its innermost crossing of the y-axis, marked with a red circle in Figure 3(a). The fiducial point has $m_0(0) = 1, m_1(0) = 3$ and is located at an (x, y) Cartesian coordinate $(0, b(0) = \frac{\alpha}{2} (1 + 3\phi))$. Figure 3 of [4] shows the next five larger members of this family, each scaled up approximately ϕ^2 in size and rotated by 36° from its predecessor. All are a $T(5, 3)$ torus knot with $N_s = 10$ self-crossings. Enumerating successive members of the $\{1, 3\}$ family with the integer index i , the parameters defining their $N_c(i)$, $b(i)$, and $L(i)$ values are tabulated in Figure 3(a) for the first six family members.

After some effort and adaptation of sequences found in the OEIS [1], it can be shown that the family’s crossing numbers for $0 \leq i \leq 5$ are given empirically by $N_c(i) = 10(37F_{2i+1} + 23F_{2i} - 3)$, where F_j is the j th Fibonacci number defined such that $F_0 = 0$. The $2i$ -dependence of the Fibonacci terms in $N_c(i)$ assures that $\lim_{i \rightarrow \infty} \frac{N_c(i+1)}{N_c(i)} = \phi^2$, as was qualitatively observed in [4]. Similarly, the fiducial point locations, $b(i)$, and strand lengths, $L(i)$, for the $\{1, 3\}$ family with $0 \leq i \leq 5$ are empirically given by the following sequences:

$$b(i) = \frac{a}{2} [m_0(i) + \phi m_1(i)], \text{ where: } m_0(i) = (-1)^i (2F_{2i+1} - 1) \quad m_1(i) = (-1)^i (2F_{2i+2} + 1)$$

$$L(i) = \frac{a}{2} [n_0(i) + \phi n_1(i)], \text{ where: } n_0(i) = 20(4F_{2i+1} + F_{2i} - 3) \quad n_1(i) = 10(8F_{2i+2} + 2F_{2i+1} + 3) .$$

Note that the $(-1)^i$ factor in m_0 and m_1 arises from the 36° rotation of the orientation of successive family members about the star axiom origin.

Although these sequences were obtained empirically for the first six family members, I conjecture there is no limit to the number of $\{1, 3\}$ family members and the applicability of these equations for their $N_c(i)$, $b(i)$, and $L(i)$ values. Consistent with the incremental ϕ^2 scaling of successive family members qualitatively reported in [4], we see that $\lim_{i \rightarrow \infty} \frac{b(i+1)}{b(i)} = \lim_{i \rightarrow \infty} \frac{L(i+1)}{L(i)} = \phi^2$. Also note that $\lim_{i \rightarrow \infty} \frac{m_1(i)}{m_0(i)} = \lim_{i \rightarrow \infty} \frac{n_1(i)}{n_0(i)} = \phi$; the asymptotic ratio of the long:short ($\phi:1$) distance metrics appears to be a direct analog to the well-known ϕ ratio for the number of kites:darts, long:short Conway worm “bow ties”, and long:short spacings of Ammann bars observed in Penrose tilings [7]. These asymptotic limits for strand properties are common to all the families described in this paper.

The $\{-1, 2\}$ family. The cyan strand highlighted on the right side of Figure 2 is the $i = 0$ member of this family with a crossing number $N_c(0) = 670$, and is shown fully in Figure 3(b). The tiling in [4] is large enough to completely contain the first 5 members of this family. They have similar shapes and all are a $T(5, 2)$ torus knot with $N_s = 5$. Their quantifying parameters are given in Figure 3(b) and obey the sequences $N_c(i) = 10(71F_{2i+1} + 44F_{2i} - 4)$, $m_0(i) = (-1)^i (2F_{2i+1} - 2F_{2i} - 3)$, $m_1(i) = (-1)^i (2F_{2i+2} - 2F_{2i+1} + 2)$, $n_0(i) = 20(7F_{2i+1} + 3F_{2i} - 4)$, and $n_1(i) = 20(7F_{2i+2} + 3F_{2i+1} + 2)$.

The $\{13, 21\}$ family. Figure 4(a) (and Figure 5(c) of [4]) shows the $i = 0$ member of this family. As described in [4], the trajectories of strands in this family have a “pretzel” feature at their inner excursion and a distinctive “bear” feature at their outer excursion. These strands are an alternating knot with $N_s = 45$ self-crossings. Visual inspection, and analysis of the knot’s Dowker-Thistlewaite (DT) notation [9][11], shows this is a non-prime knot consisting of a connected sum of five trefoil knots (the inner pretzels) and five $T(5, 2)$ torus knots (the bears). Qualitatively, each successive member grows in size by a factor of approximately ϕ^2 , is rotated by 36° , and has additional oscillations in “wavy” portions of the strand (for example, those connecting the pretzel to the bear). Despite the systematic development of these fractal oscillations, the quantifying parameters tabulated in Figure 4(a) obey the sequences $N_c(i) = 10(64F_{2i+7} + 2F_{2i} - 20i - 81)$, $m_0(i) = (-1)^i (4F_{2i+4} + 2F_{2i} + 1)$, $m_1(i) = (-1)^i (4F_{2i+5} + 2F_{2i+1} - 1)$, $n_0(i) = 40(37F_{2i+1} + 24F_{2i} - 10i - 28)$, and $n_1(i) = 20(74F_{2i+2} + 48F_{2i+1} + 10i + 23)$.

The $\{5, 11\}$ family. Figure 4(b) shows the $i = 0$ member of this family. These strands are a non-alternating knot projection with $N_s = 20$ self-crossings. KnotInfo [11] is unable identify the knot using this projection’s DT notation. Qualitatively, each successive member shows the usual progression of size and rotational orientation, and shows additional fractal oscillations in “wavy” portions of the strand. The quantifying parameters tabulated in Figure 4(b) obey the sequences $N_c(i) = 10(43F_{2i+5} + 4F_{2i} - 4i - 18)$, $m_0(i) = (-1)^i (2F_{2i+5} - 5)$, $m_1(i) = (-1)^i (2F_{2i+6} - 5)$, $n_0(i) = 20(20F_{2i+1} + 11F_{2i} - 4i - 13)$, and $n_1(i) = 10(40F_{2i+2} + 22F_{2i+1} + 4i + 11)$.

The $\{-7, -11\}$ family. Figure 4(c) shows the $i = 0$ member of this family. These strands are an alternating knot with $N_s = 30$ self-crossings. Analysis of its DT notation [11] reveals it to be a connected sum of five trefoil knots (the inner pretzels) and a $T(15, 2)$ torus knot (periodic knot $15a_{85263}$ [10]). Successive members of this family develop 10 fractal “tower” structures at the outer extrema of their trajectory, as shown in Figure 5(a) of [4]. The quantifying parameters tabulated in Figure 4(c) obey the sequences $N_c(i) = 10(25F_{2i+6} + 3F_{2i+1} - 8i - 53)$, $m_0(i) = (-1)^{i+1} (6F_{2i+2} + 1)$, $m_1(i) = (-1)^{i+1} (6F_{2i+3} - 1)$, $n_0(i) = 20(16F_{2i+1} + 15F_{2i} - 8i - 19)$, and $n_1(i) = 10(32F_{2i+2} + 30F_{2i+1} + 8i + 5)$.

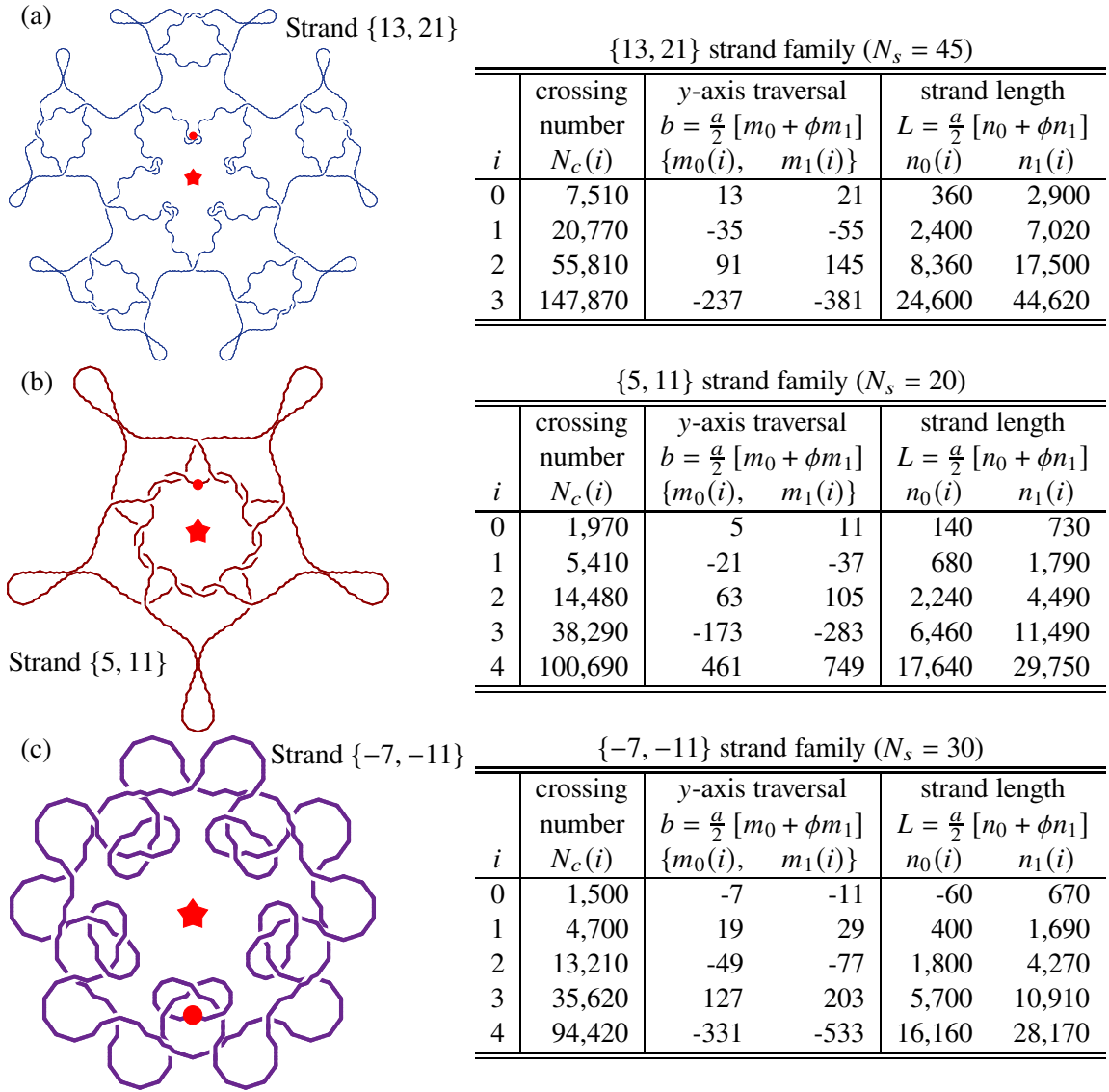


Figure 4: (a) First ($i = 0$) members and quantifying parameters of the (a) {13, 21}, (b) {5, 11}, and (c) {-7, -11} strand families. The locations of strand fiducial points are labeled with red circles.

The {5, 7} family. This family is distinct from those described previously in that the smallest member has a different knot topology than that of subsequent members. Figure 5(a) shows the $i = 0$ member is a non-alternating knot projection with $N_s = 50$ self-crossings. Figure 5(b) shows the $i = 1$ member. Members with $i \geq 1$ are a non-alternating knot projection with $N_s = 70$ self-crossings. The additional 20 self-crossings for $i \geq 1$ members arise from the development of a fractal tower feature which becomes entangled in the outer pretzel crossing in the trajectory of the $i = 0$ member. This tower ultimately becomes an extremum in the trajectory of strands with large values of i . Members with $0 \leq i \leq 5$ are shown in Figure 4 of [4], which shows the growth of the fractal tower. KnotInfo [11] is unable to identify these two knots from their projection's DT notation. Despite the tower development and change in knot topology, the quantifying parameters tabulated in Figure 5 obey one set of sequences: $N_c(i) = 10(92F_{2i+3} + 22F_{2i} - 4i - 31)$, $m_0(i) = (-1)^i(4F_{2i+2} + 1)$, $m_1(i) = (-1)^i(4F_{2i+3} - 1)$, $n_0(i) = 40(9F_{2i+1} + 4F_{2i} - 2i - 7)$, and $n_1(i) = 10(36F_{2i+2} + 16F_{2i+1} + 4i + 7)$.

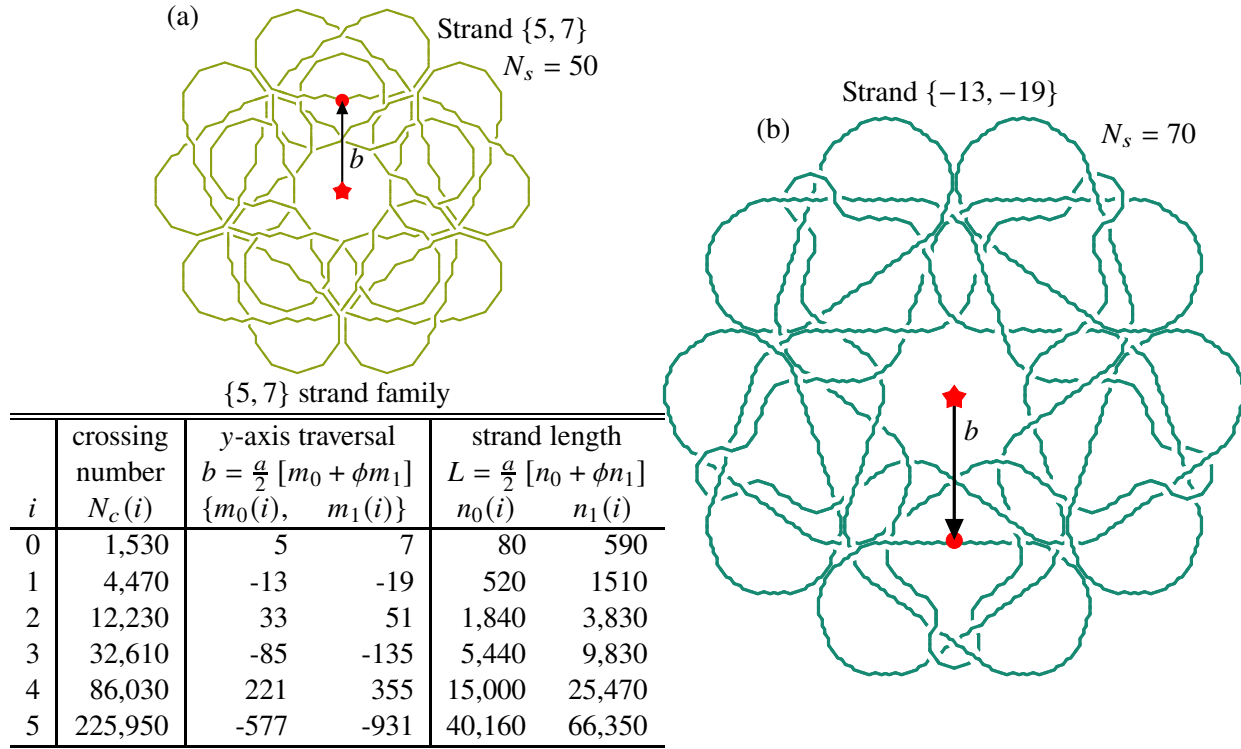


Figure 5: (a) First ($i = 0$) and (b) second ($i = 1$) members of the $\{5, 7\}$ strand family.

Conclusions and Discussion

Medieval Girih-decorated periodic tilings typically contain less than four, quite simple, strand shapes [8] woven into interlaced strapwork patterns of an ordered aesthetic seen throughout Islamic art and architecture. In contrast, the aperiodic Girih pattern in Figure 2 reflects the seeming chaos of the Penrose tiling, with a distinctive beauty emerging in what may be an infinite variety of strand structures. When extracted from the strapwork pattern, these strands have an aesthetic appeal ranging from that of simple pentamerous flowers to complex pentagonal snowflake analogs. That the strands form mathematical knots only adds to their interest; the aperiodic Girih pattern is a veritable factory of complex knots and links, and many of their properties, including their periodicity and chirality, remain unexplored.

Lacking an analytic theory to predict strand shapes, I instead describe regularity in the quantitative properties and topologies of a small subset of strands orbiting the center of a star axiom tiling. When grouped into families of the same knot topology and similar shape, the location (b), size (L), and crossing number (N_c) of successive members, i , of family members obey empirical sequences I conjecture to hold throughout the infinite pattern as $i \rightarrow \infty$. I offer a few observations to support this conjecture: (1) As noted earlier, ratios of consecutive sequence values asymptotically approach ϕ^2 , consistent with scaling laws that would be expected in Penrose tilings. (2) The locations of incomplete strands in these families that extend beyond the periphery of this finite tiling are observed to be consistent with the sequence predictions. (3) A future report will show that, for at least some strand families, use of these sequences with half-integral i values correctly gives $L(i)$ and $N_c(i)$ for “missing” strands having the family’s characteristic shape and knot topology, but that orbit local sun vertex neighborhoods [7] distributed throughout the finite tiling studied here.

Though not described in this report, I observe that successive family members are often related by systematic inflation of Girih strand segments trapped within the linear Conway worms that are pervasive in

Penrose P2 tilings. Conway worms consist of long and short bow tie structures concatenated in musical sequences that have inflation properties closely connected to the Fibonacci sequence [7]. It is thus unsurprising that terms containing Fibonacci sequences appear in the empirical expressions for $N_c(i)$, $b(i)$, and $L(i)$. Additionally, it is observed that terms linearly dependent on i only appear in $N_c(i)$ and $L(i)$ for strand families which develop successive fractal structures (e.g. the $\{13, 21\}$, $\{5, 11\}$, $\{-7, -11\}$, and $\{5, 7\}$ families). Though beyond the scope of this report, detailed study of the inflation of strand sub-structures yields an analytic scheme to obtain the sequences that quantify $L(i)$ for many strand families.

Finally, it should be noted that strand shapes are sensitive to long-range organizing principles of the Penrose tiling. The well-known local isomorphism theorem of Conway states that every local region of radius d is replicated an infinite number of times through a Penrose tiling, and that the region's closest replica lies at a distance of no more than $d\phi^3/2$ away [6]. The shapes of smaller Girih strands probe the boundaries of such local regions, and large, delocalized strands probe the linkages among adjoining regions. For example, consider a local region containing strands orbiting a star vertex neighborhood. The region's size and its interactions with adjacent local regions can be probed by perturbations in the shapes of the unperturbed "star axiom" strands described here. These "perturbed" strands are one contribution to the rich variety of strand shapes to be found in the aperiodic Girih pattern, and will be the topic of future reporting.

References

- [1] *The On-Line Encyclopedia of Integer Sequences*, published electronically at <https://oeis.org>, 2010. The Fibonacci sequence used here follows the convention in Sequence A000045.
- [2] J. Bonner and C. Kaplan. *Islamic Geometric Patterns*. Springer Nature, 2017.
- [3] E. Broug. *Islamic Geometric Design*. London: Thames & Hudson, 2013. ch. 2.
- [4] J. Cline. "Interlace Patterns Emerging in a Penrose-Type Islamic Design." *Proceedings of Bridges 2024: Mathematics, Art, Music, Architecture, Culture*. H. Verrill, K. Kattchee, S. L. Gould, and E. Torrence, Eds. Phoenix, Arizona: Tessellations Publishing, 2024. pp. 163–170. <http://archive.bridgesmathart.org/2024/bridges2024-163.html>.
- [5] M. Gardner. "Mathematical Games: Extraordinary nonperiodic tiling that enriches the theory of tiles." *Scientific American*, vol. 236, no. 1, 1977, pp. 110–121. <http://www.jstor.org/stable/24953856>.
- [6] M. Gardner. *Penrose Tiles to Trapdoor Ciphers...and the Return of Dr Matrix*. Washington, D. C.: The Mathematical Association of America, 1997. p. 6.
- [7] B. Grünbaum and G. C. Shephard. *Tilings and Patterns*. New York, N. Y.: W. H. Freeman, 1987. ch. 10.3, 10.5.
- [8] B. Grünbaum and G. C. Shephard. "Interlace Patterns in Islamic and Moorish Art." *Leonardo*, vol. 25, no. 3, 1992, pp. 331–339.
- [9] J. Hoste, M. Thistlethwaite, and J. Weeks. "The first 1,701,936 knots." *The Mathematical Intelligencer*, vol. 20, 1998, pp. 33–48.
- [10] S. Jakuba and S. Naik. "Periodic knots and Heegaard Floer correction terms." *J. Eur. Math. Soc.*, vol. 18, 2016.
- [11] C. Livingston and A. H. Moore. "KnotInfo: Table of Knot Invariants." URL: knotinfo.math.indiana.edu. January 2025.
- [12] V. Ostromoukhov. "Mathematical tools for computer-generated ornamental patterns." *Electronic Publishing, Artistic Imaging, and Digital Typography*. R. D. Hersch, J. André, and H. Brown, Eds. Berlin, Heidelberg: Springer Berlin Heidelberg, 1998. pp. 193–223.